Cell Reports

Report

Genetic Isolation of Hypothalamic Neurons that Regulate Context-Specific Male Social Behavior

Graphical Abstract

Authors

Marta E. Soden, Samara M. Miller, Lauren M. Burgeno, Paul E.M. Phillips, Thomas S. Hnasko, Larry S. Zweifel

Correspondence

larryz@uw.edu

In Brief

Soden et al. characterize a population of neurons in the ventral premammillary nucleus of the hypothalamus that are genetically defined as dopaminergic but that do not release detectable dopamine. These neurons are activated in specific social contexts and function via glutamate release to regulate male same-sex social interactions.

Highlights

- A group of neurons in the ventral premammillary nucleus express dopamine markers
- These neurons are activated in male intruder, but not resident, mice
- These neurons regulate same-sex social behavior in specific contexts
- These neurons function via glutamate release, but do not release detectable dopamine

Soden et al., 2016, Cell Reports *16*, 1–10
July 12, 2016
http://dx.doi.org/10.1016/j.celrep.2016.05.067

CellPress

Please cite this article in press as: Soden et al., Genetic Isolation of Hypothalamic Neurons that Regulate Context-Specific Male Social Behavior, Cell Reports (2016), http://dx.doi.org/10.1016/j.celrep.2016.05.067

Cell Reports
Report

Genetic Isolation of Hypothalamic Neurons that Regulate Context-Specific Male Social Behavior

Marta E. Soden,[1,2] Samara M. Miller,[1,2] Lauren M. Burgeno,[1,2] Paul E.M. Phillips,[1,2] Thomas S. Hnasko,[3] and Larry S. Zweifel[1,2,*]
[1]Department of Pharmacology, University of Washington, Seattle, WA 98195, USA
[2]Department of Psychiatry and Behavioral Sciences, University of Washington, Seattle, WA 98195, USA
[3]Department of Neurosciences, University of California, San Diego, La Jolla, CA 92093, USA
*Correspondence: larryz@uw.edu
http://dx.doi.org/10.1016/j.celrep.2016.05.067

SUMMARY

Nearly all animals engage in a complex assortment of social behaviors that are essential for the survival of the species. In mammals, these behaviors are regulated by sub-nuclei within the hypothalamus, but the specific cell types within these nuclei responsible for coordinating behavior in distinct contexts are only beginning to be resolved. Here, we identify a population of neurons in the ventral premammillary nucleus of the hypothalamus (PM_V) that are strongly activated in male intruder mice in response to a larger resident male but that are not responsive to females. Using a combination of molecular and genetic approaches, we demonstrate that these PM_V neurons regulate intruder-specific male social behavior and social novelty recognition in a manner dependent on synaptic release of the excitatory neurotransmitter glutamate. These data provide direct evidence for a unique population of neurons that regulate social behaviors in specific contexts.

INTRODUCTION

In rodents, olfactory information is a major modality for social communication. Inputs from the main olfactory bulb and accessory olfactory bulb directly innervate sub-nuclei of the medial amygdala that transmit this information to the hypothalamus (Scalia and Winans, 1975; Kevetter and Winans, 1981; Choi et al., 2005; Sosulski et al., 2011). The hypothalamus also receives direct olfactory information relevant to social cues (Yoon et al., 2005). Hypothalamic sub-populations have been identified within the ventrolateral ventromedial hypothalamus (VMH_{VL}) that regulate key social behaviors, including aggressive responses to conspecific threats and mating (Lin et al., 2011; Lee et al., 2014). Neurons within the medial pre-optic area (MPO) of the hypothalamus have also been isolated in mice and shown to regulate parental care or agression toward pups, depending on the animals' sexual experience (Wu et al., 2014). Numerous other sub-nuclei within the hypothalamus have been implicated in the regulation of social behaviors (Swanson, 2000), but virtually nothing is known about the cell types within these regions that contribute to these behaviors.

The ventral premammillary nucleus of the hypothalamus (PM_V) is highly connected with the brain's social networks (Canteras et al., 1992; Swanson, 2000; Cavalcante et al., 2014), and mapping studies using the immediate early gene *Fos* demonstrated that PM_V neurons are activated in multiple social contexts (Cavalcante et al., 2006; Borelli et al., 2009; Motta et al., 2009; Donato et al., 2010, 2013). Early analysis of the catecholamine-producing neurons of the brain identified a non-canonical dopamine neuron population within the PM_V (Hedreen, 1978; Meister and Elde, 1993; Zoli et al., 1993), but whether these neurons regulate social behavior and whether they use dopamine as a neurotransmitter is not known. Based on previous evidence that neurons in the PM_V express mRNA for the dopamine transporter (DAT; Meister and Elde, 1993), we used DAT as a genetic marker to isolate this population. We demonstrate that PM_V-DAT neurons are connected to brain regions implicated in conspecific social behavior and are principally glutamatergic, but do not release detectable dopamine. We show that PM_V-DAT neurons are most highly activated when male mice are intruders into the residence of a larger male. Chemogenetic inhibition of PM_V-DAT neurons specifically reduces exploratory social behavior in intruder males and impairs social novelty recognition. Activation of PM_V-DAT neurons increases exploratory social investigation of familiar mice in a manner dependent on synaptic glutamate release. Our genetic isolation and characterization of this unique neuronal population provides direct evidence for a hypothalamic cell type that regulates male intruder behavior and social novelty in specific contexts.

RESULTS

Genetic Isolation of PM_V-DAT Neurons

Given the previous identification of neurons in the PM_V that express DAT (Hedreen, 1978; Meister and Elde, 1993), we sought to determine the function of these neurons within social contexts. To confirm the presence of these neurons, we performed a differential search of the Allen Institute for Brain Science Mouse Brain Atlas in situ hybridization data (Lein et al., 2007). Three of

Please cite this article in press as: Soden et al., Genetic Isolation of Hypothalamic Neurons that Regulate Context-Specific Male Social Behavior, Cell Reports (2016), http://dx.doi.org/10.1016/j.celrep.2016.05.067

the top 30 genes enriched in the PM_V are canonical markers for the synthesis and release of the neurotransmitter dopamine: dopamine transporter (DAT; *Slc6a3*), dopa-decarboxylase (DDC; *Ddc*), and the vesicular monoamine transporter (VMAT; *Slc18a2*). Of these markers, DAT appeared to be the most selective for the PM_V within the hypothalamus. Based on this observation, along with previous data demonstrating DAT mRNA in the PM_V (Meister and Elde, 1993) and observations that mice expressing Cre recombinase from the DAT locus are the most reliable for isolating dopamine-producing neurons (Lammel et al., 2015), we genetically isolated PM_V-DAT neurons utilizing the DAT-Cre mouse line ($Slc6a3^{Cre/+}$; Zhuang et al., 2005). To validate the expression data from the Mouse Brain Atlas, we performed immuno-isolation of actively translating mRNA using RiboTag mice (Sanz et al., 2009). These mice allow for Cre-dependent expression of an affinity-tagged ribosomal protein, Rpl22-HA, and subsequent immunoprecipitation (IP) of polyribosomes. $Slc6a3^{Cre/+};Rpl22^{HA/+}$ mice were used to isolate mRNA from DAT neurons in the PM_V following microdissection (Figures 1A–1C). We observed a significant enrichment of *Slc6a3*, *Ddc*, *Slc18a2*, and tyrosine hydroxylase (*Th*) mRNA in the IP relative to the input, which contains mRNA from all cell types in the region (Figure 1D). Similar enrichment of these markers was observed when mRNA was isolated from canonical dopamine neurons in the ventral tegmental area (VTA) of $Slc6a3^{Cre/+};Rpl22^{HA/+}$ mice (Figures S1A and S1B).

Quantification of PM_V-DAT neurons revealed that these cells make up 25% of neurons in this region (952 YFP+ cells/3767 NeuN+ cells, alternate sections counted from three mice; Figure S1C). Connectivity mapping of PM_V-DAT neurons through conditional expression of an EGFP-tagged synaptic marker protein synaptophysin-EGFP (AAV1-FLEX-synapto-EGFP) revealed axonal projections to numerous downstream targets previously implicated in the regulation of social behavior (Canteras et al., 1992). These included the VMH_{VL}, the MPO, the medial postero-ventral subdivision of the medial amygdala (MeA_{PV}), the amygdalo-hippocampal region of the medial amygdala (MeA_{AHi}), the postero-dorsal and ventral subdivisions of bed nucleus of the stria-terminalis ($BNST_{PD}$ and $BNST_{PV}$), the anterior hypothalamic nucleus (AHN), and the periaqueductal gray (PAG; Figure 1E). Analysis of PM_V-DAT projections obtained from the Allen Brain Institute Mouse Connectivity Atlas (Oh et al., 2014) revealed similar results. To establish the density of PM_V-DAT projections to various targets, we generated an analysis program to quantify fluorescent pixels in target areas using data from the Connectivity Atlas. While the BNST received the most total input, the densest innervation was observed in the VMH_{VL} (Figure S1D).

PM_V-DAT Neurons Release Glutamate, but Not Detectable Dopamine

Although previous studies have demonstrated the presence of 6-OH-DA-sensitive neurons in the PM_V (Hedreen, 1978), these neurons were not immunoreactive for dopamine (Zoli et al., 1993). To test whether PM_V-DAT neurons release detectable dopamine, we expressed ChR2 in PM_V-DAT neurons and assayed for light-evoked dopamine release using fast-scan cyclic voltammetry (FSCV) in acute slices from multiple target regions (VMH_{VL}, MeA_{MPV}, and BNST). We did not detect any dopamine transients following optical stimulation of PM_V-DAT fibers using multiple stimulus parameters (5, 10, 20, and 30 Hz; Figures 2A and 2B). In contrast, expression of ChR2-mCherry in VTA dopamine neurons and optical stimulation of terminals in the nucleus accumbens resulted in robust dopamine release (Figures 2A and 2B). Pre-treating mice with L-DOPA, the dopamine precursor shown to be transported by PM_V neurons (Zoli et al., 1993), did not enhance detection of dopamine release (Figures 2A and 2B). These data do not rule out that dopamine may be released below the level of detection of FSCV. However, consistent with our FSCV results, we did not detect any protein for TH or DAT in the cell bodies or terminal fields of DAT-PM_V neurons using immunohistochemistry (Figures S2A and S2B).

Because we detected mRNA, but no protein, for dopamine markers in PM_V-DAT neurons, we compared the relative amounts of mRNA for these markers in PM_V-DAT neurons versus VTA-DAT neurons using the IP fractions from our RiboTag analysis. Although mRNA for dopaminergic markers is highly enriched in PM_V-DAT neurons relative to other neurons within the region, these cells contained only 5%–10% the amount of dopaminergic mRNAs compared to VTA-DAT neurons (Figure S2C). In contrast, PM_V-DAT neurons contained three times as much mRNA encoding the vesicular glutamate transporter vGluT2 (*Slc17a6*) as did VTA-DAT neurons. Additional electrophysiological analysis of PM_V-DAT neurons revealed that these neurons do not share common electrophysiological properties with VTA dopaminergic neurons (Figures 2C–2G and S2D–S2G), indicating that these neurons are a unique population.

Consistent with the detection of mRNA encoding vGluT2, analysis of synaptic connectivity in the VMH_{VL} (Figure 2H) revealed the majority of light-evoked responses from ChR2-expressing terminals of PM_V-DAT neurons are monosynaptic excitatory currents blocked by the glutamatergic antagonist CNQX (Figure 2I). Delayed and unsynchronized inhibitory and excitatory currents were also seen in a small number of cells (five inhibitory, seven excitatory; Figures 2J and 2K). A smaller sample of recordings from the BNST (n = 6/15 cells connected) and MPN (n = 9/14 cells connected) produced similar results.

PM_V-DAT Neurons Regulate Context-Specific Social Behavior

To confirm previous observations of *Fos* induction in the PM_V following exposure of animals to opposite- and same-sex odorants (Cavalcante et al., 2006; Leshan et al., 2009; Donato et al., 2010), we exposed male and female mice to clean bedding (control) or bedding soiled by a same-sex or opposite-sex mouse, followed by immunohistochemistry for Fos. We observed a modest increase in Fos protein in response to opposite-sex odorants in male and female mice. However, male, but not female, mice showed increased Fos in response to same-sex odorants that was significantly higher than Fos observed in response to opposite-sex odorants (Figures S3A–S3C).

To establish whether PM_V-DAT neurons are activated in male mice in a context-dependent manner, we quantified Fos expression in virally labeled cells. Mice were exposed to one of five social encounter conditions: no encounter (control), intruder into the cage of a male resident, intruder into the cage of a female resident, resident exposed to a male intruder, and resident

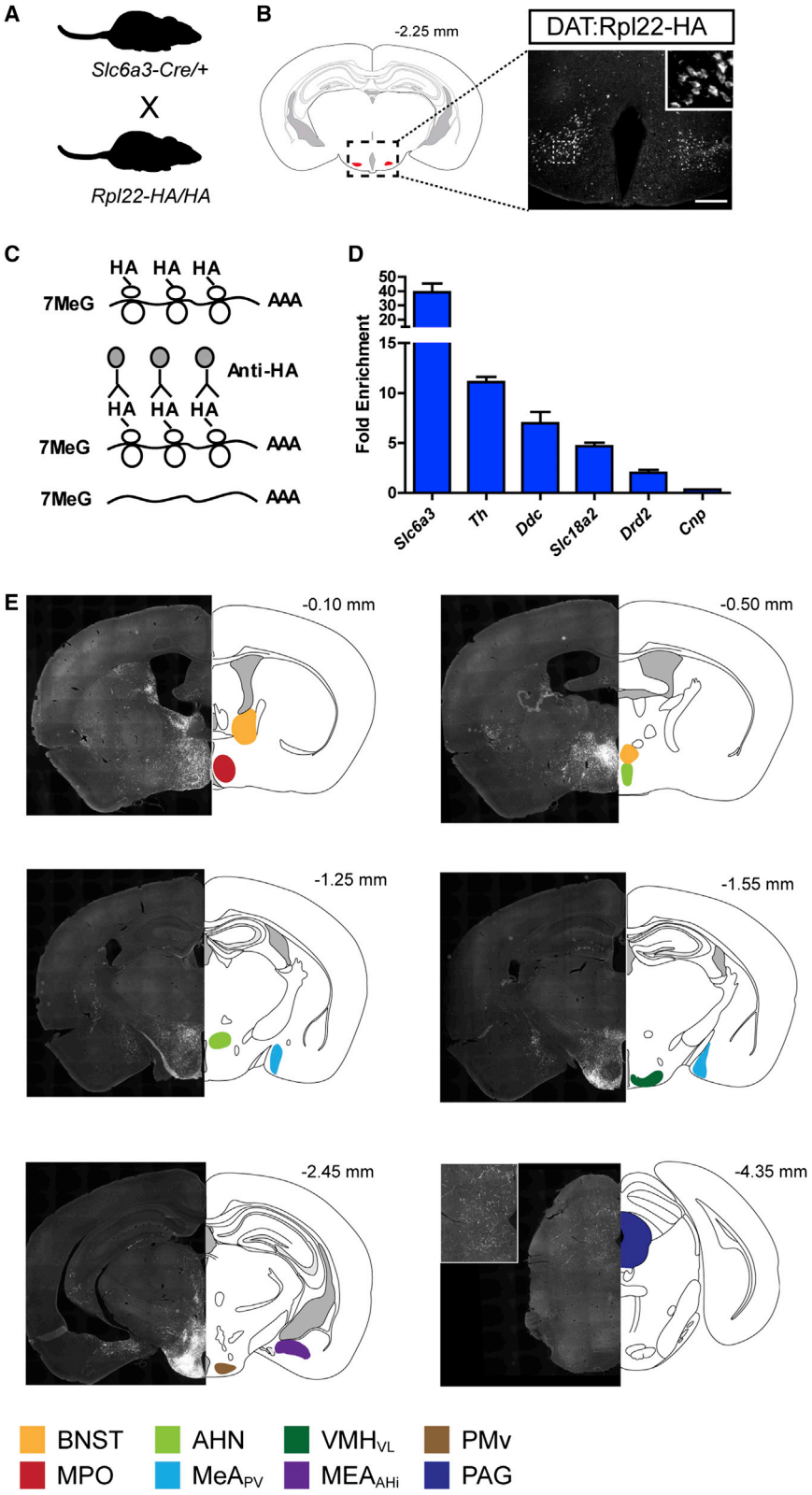

Figure 1. Molecular Profile and Connectivity of PM_V-DAT Neurons

(A) Schematic generation of DAT-Cre-RiboTag mice.

(B) Atlas image depicting the PM_V; boxed region is depicted in immunohistochemistry image of Rpl22-HA (right) and inset. Scale bar, 250 μm.

(C) Cartoon depicting RiboTag technique: in Cre-positive cells the ribosomal protein Rpl22 is labeled with an HA tag; immunoprecipitation of HA isolates ribosome-associated mRNAs.

(D) Fold enrichment (IP compared to input) of specific mRNAs isolated from PM_V-DAT neurons (n = 3 pooled samples, each from 2–3 mice).

(E) Projections of PM_V-DAT neurons are revealed by expression of synapto-EGFP in axon terminals. Atlas images show approximate distance from bregma; indicated brain regions are color-coded. See also Figure S1.

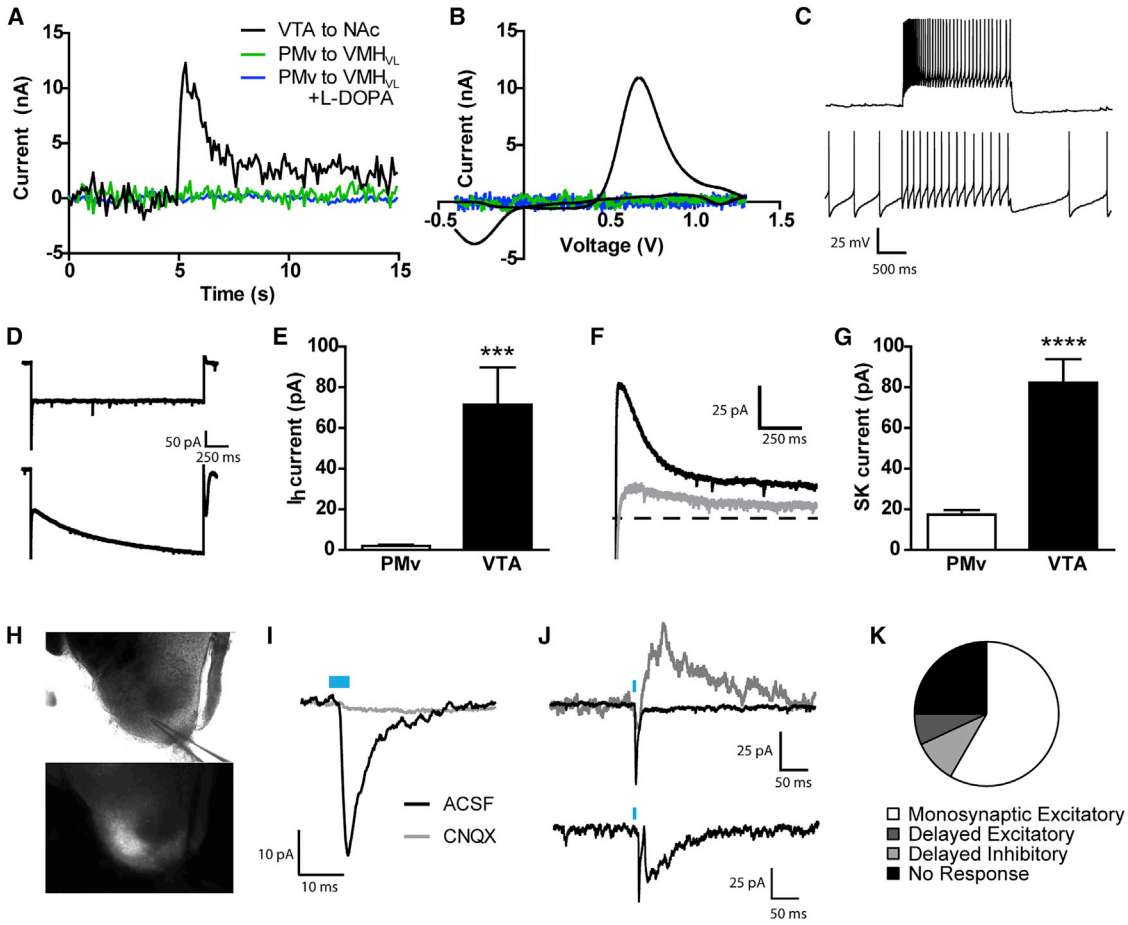

Figure 2. PM$_V$-DAT Neurons Are Principally Glutamatergic and Do Not Release Dopamine

(A and B) Example traces (A) and current/voltage plots (B) showing light-evoked dopamine release detected using FSCV in control slices expressing ChR2 in VTA-DAT neurons, recording in the NAc. No signal was detected in the VMH$_{VL}$ when ChR2 was expressed in PM$_V$-DAT neurons, even with pre-loading of L-DOPA.

(C) Example traces showing that PM$_V$-DAT neurons did not spontaneously fire in slice but did fire accommodating action potentials with current injection (top trace), while VTA-DAT neurons did fire spontaneously (bottom trace).

(D and E) Example traces (D) and quantification (E) of I_h current in PM$_V$-DAT neurons (top) and VTA-DAT neurons (bottom).

(F and G) Example traces (F) and quantification (G) of SK currents in PM$_V$-DAT neurons (gray) and VTA-DAT neurons (black).

(H) DIC (top) and fluorescent (bottom) images of an acute slice with fluorescent ChR2-mCherry fibers in the VMH$_{VL}$ and patch electrode visible. Scale bar, 250 μm.

(I) Example trace of EPSC in the VMH$_{VL}$ evoked by 5-ms blue light stimulation; the EPSC could be blocked by bath application of CNQX (10 μM).

(J) Top: example recordings showing a light-evoked monosynaptic EPSC (black trace, holding at −60 mV) and a delayed, unsynchronized IPSC (gray trace, holding at 0 mV). Bottom: example recording showing a light-evoked monosynaptic EPSC (initial fast depolarization) and a delayed, unsynchronized EPSC. All traces are averages of 15 sweeps.

(K) Proportion of VMH$_{VL}$ neurons recorded that received each type of synaptic input.

See also Figure S2.

exposed to a female intruder. Fos levels in PM$_V$-DAT neurons were significantly higher in male same-sex intruders relative to all other contexts (Figures 3A and 3B). PM$_V$-DAT neurons were a subset of the total Fos+ PM$_V$ neurons, but were comprised of a significantly larger subset in the same-sex intruder context compared to other contexts (Figure S3D). To test whether Fos activation in male intruder mice was primarily driven by the odorant context of the resident cage or by the resident mouse itself, we measured Fos in an ''intruder'' male following an encounter with a ''resident-like'' male (i.e., larger, singly housed, sexually experienced) in a neutral environment (clean cage). Fos in PM$_V$-DAT neurons was only modestly activated in this context (Figures 3A and 3B), indicating that contextual odorants play a large role in driving PM$_V$-DAT activation in intruder mice.

Our observation that PM$_V$-DAT neurons are most strongly activated in male mice when these animals are intruders is consistent with previous reports (Borelli et al., 2009; Motta et al., 2009) and suggests that these neurons may preferentially function within this context. To test this hypothesis, we selectively attenuated the activity of PM$_V$-DAT neurons through conditional expression of the inhibitory DREADD receptor hM4Di (AAV1-FLEX-hM4Di-YFP). Consistent with previous reports (Armbruster et al., 2007), activation of hM4Di by the selective agonist clozapine-N-oxide (CNO) reduced the excitability of PM$_V$-DAT

neurons (Figures S3E–S3H). Behavioral analysis of hM4Di and control mice (AAV1-FLEX-mCherry) revealed that reduced excitability of PM_V-DAT neurons was associated with a significant reduction in social investigation (anogenital sniffing, oral-facial sniffing, and grooming) by male intruder mice, but had no effect on resident male behavior or on male response to females. An encounter with a ''resident-like'' male in a neutral cage was also not affected (Figures 3C–3E and S3I).

A reduction in social exploratory behavior by intruder mice may represent a deficit in social recognition within this context. To test this hypothesis, we analyzed behavior in a three-chamber social preference and social recognition assay. Reduced excitability of PM_V-DAT neurons through hM4Di activation did not alter behavioral preference for a novel mouse versus a novel object, but did reduce social recognition of a novel versus familiar mouse (Figures 3F–3G and S3J–S3K).

PM_V-DAT Neurons Regulate Social Behavior through Glutamate Release

To further investigate the extent to which activation of PM_V-DAT neurons influences social recognition and social investigation, we developed a co-habitation assay to monitor social investigation of a familiar cage-mate, while PM_V-DAT neurons are selectively activated using the light-activated ion channel ChR2. Because PM_V-DAT neurons should be minimally activated in this context, this assay allowed us to establish the sufficiency of activation of PM_V-DAT neurons for social investigation behaviors.

To determine the optimal stimulation parameters for this assay, we analyzed the synaptic fidelity of light-evoked action potentials in postsynaptic VMH_{VL} neurons using a common stimulation paradigm (5-ms light stimuli at 20 Hz). Fidelity diminished with repetitive stimulation at this frequency (Figure S4A). This decrease was not observed when action potential firing was recorded in PM_V-DAT neuron cell bodies (Figure S4B). Quantitative analysis of light-evoked postsynaptic currents confirmed a significant synaptic rundown at frequencies of 5 Hz and above (Figures S4C and S4D), suggesting that low-frequency stimulation in these neurons is optimal for maintaining synaptic connectivity.

To monitor exploratory social behavior between familiar mice, we tested conspecific males co-housed from birth. One mouse was surgically injected with either AAV1-FLEX-ChR2-mCherry or AAV1-FLEX-mCherry and a fiber-optic was implanted above the PM_V (Figure 4A). Mice were assayed for investigatory behavior of their cage-mate with or without optical stimulation (Figure 4B). While 3-Hz light stimulation had no effect on social interaction in control mice, mice expressing ChR2 significantly increased social investigation (anogenital sniffing, oral-facial sniffing, and grooming) of their cage-mate during light stimulation (Figures 4C and S4E). Light stimulation had no effect on exploration of a familiar object in the home cage (Figure 4D) and did not affect distance traveled in the cage (Figure S4F). Light stimulation also had no effect in a real-time place preference (RTPP) assay, suggesting that activation of the PM_V is neither rewarding nor aversive (Figure 4E). Finally, light stimulation did not affect behavior in an open-field assay (Figures S4G and S4H), indicating no overt role for PM_V-DAT neurons in regulating anxiety.

To further establish the extent to which activation of PM_V-DAT neurons can enhance social investigation, we stimulated PM_V-DAT neurons in resident animals, a context in which PM_V-DAT neurons are not robustly activated, but in which animals are already actively engaged in social investigation. We observed an increase in investigation time in ChR2-expressing animals, indicating that artificially activating PM_V-DAT neurons can drive increased social behavior even when animals are already socially engaged (Figure S4I). In contrast, stimulation of PM_V-DAT neurons in intruder mice did not enhance social investigation (Figure S4J), indicating that these neurons are already optimally functioning in this context.

To confirm that glutamate is the critical neurotransmitter responsible for the effect of PM_V-DAT neurons on social behavior, we repeated our co-habitation experiments by expressing ChR2 in DAT-PM_V neurons in mice in which the gene encoding vGluT2, *Slc17a6*, is inactivated in dopamine neurons ($Slc6a3^{iCre/+}$; $Slc17a6^{lox/lox}$, or DAT-vGlut2 KO) (Hnasko et al., 2010). Consistent with PM_V-DAT neurons being glutamatergic, light-induced excitatory post-synaptic currents (EPSCs) were observed in control mice ($Slc6a3^{Cre/+}$; $Slc17a6^{lox/+}$), but not in DAT-vGlut2 KO mice (Figure 4F, inset). Optical stimulation of PM_V-DAT neurons significantly enhanced social investigation in control mice, but not in DAT-vGlut2 KO mice (Figure 4F). Stimulation of PM_V-DAT neurons in DAT-vGlut2 KO and control mice was not associated with increased investigation of a familiar object (Figure 4G) or with RTPP (Figure 4H).

Because DAT-vGlut2 KO mice are a loss of function, we next asked whether these mice have altered baseline social behavior in the resident-intruder assay in the absence of light stimulation. Consistent with hM4Di-mediated inhibition of PM_V-DAT neurons, DAT-vGlut2 KO mice displayed significantly reduced social exploratory behavior when they were intruders in the cage of a resident male (Figure 4I). This effect was not observed when the mice were residents in response to a male or female intruder (Figures 4J and 4K). A caveat to this approach is that genetic inactivation of vGlut2 in DAT-expressing neurons removes this protein from all such neurons, including those in the VTA. It has been demonstrated that inactivation of DAT-expressing neurons in the VTA disrupts social behavior (Gunaydin et al., 2014; Yu et al., 2014). Therefore, we inactivated DAT neurons in the VTA by expressing hM4Di in these cells (Figure S4K). Inhibition of DAT neurons in the VTA did not affect investigatory behavior in intruder mice, but did reduce this behavior in resident males toward male intruders (Figures S4L–S4N).

DISCUSSION

Our data identify a unique population of neurons in the mouse hypothalamus that regulate intruder-specific male behavior. Numerous studies have identified the hypothalamus as a key regulator of socially motivated behavior (Swanson, 2000), but, to date, a defined group of neurons specifically tuned to influence conspecific behavior exclusively in intruder males had not been demonstrated. Our observations are supported by previous findings of increased Fos in the PM_V of male intruder rats (Borelli et al., 2009; Motta et al., 2009). Motta et al. (2009) also have observed increased Fos protein in the

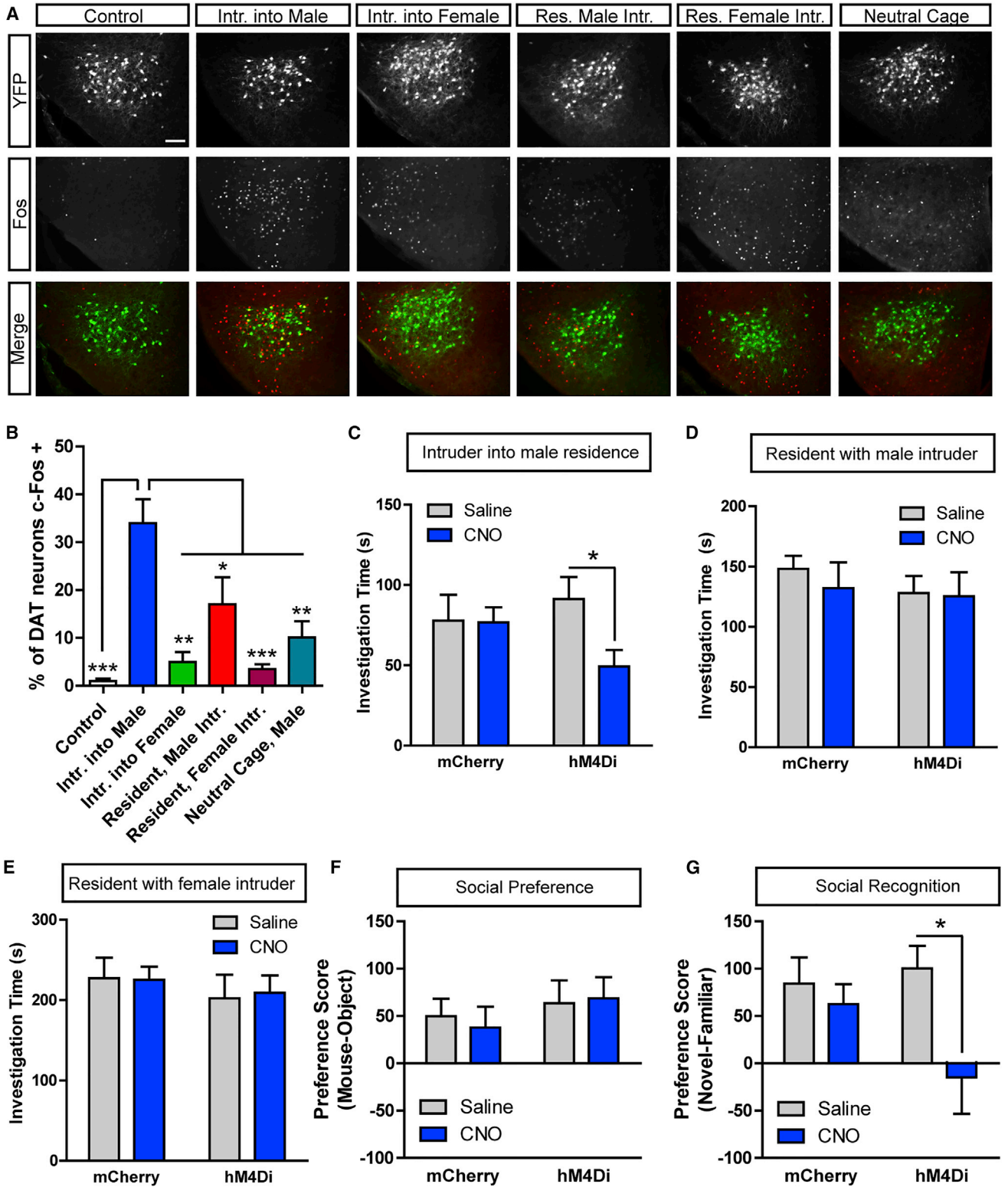

Figure 3. PM_V-DAT Neurons Regulate Intruder-Specific Behavior

(A and B) Images (A) and quantification (B) of Fos levels in PM_V-DAT neurons during social encounters (n = 3 mice/group; one-way ANOVA $F_{(5,12)} = 12.26$, $p < 0.001$; Tukey's multiple comparison *$p < 0.05$, **$p < 0.01$, ***$p < 0.001$; scale bar, 100 μm).

(legend continued on next page)

dorsal premammillary nucleus (PM_D) and found that lesioning the PM_D reduced exploratory social behavior and defensive behavior by much smaller subordinate intruder rats. These data collectively point to specific populations within the PM_V and PM_D that regulate intruder-specific behavior.

It has been reported that lesions of the PM_V increase aggressive behavior in male rats (Vandenberg et al., 1983). Since PM_V-DAT neurons only constitute approximately 25% of the total neurons of the PM_V, and numerous Fos-positive PM_V neurons in the resident-intruder assays are not DAT-positive, PM_V-DAT neurons likely are not the only population involved in context-specific social behavior. Thus, lesioning of the entire PM_V may disrupt multiple cell types that when collectively destroyed lead to different behavioral outcomes.

We also have found that optogenetic stimulation of PM_V-DAT neurons engages social exploration of a familiar mouse. These findings, together with our observations that social recognition is impaired when PM_V-DAT neurons are inhibited, suggest that these neurons influence exploration and novelty detection specific for socially relevant stimuli. Similarly, it also has been demonstrated that dopamine neurons of the VTA selectively influence social exploration, but not novelty exploration (Gunaydin et al., 2014). Interestingly, we have found that inhibition of VTA-DAT neurons reduces social behavior by resident males, but not by intruder males, and this behavior is not sensitive to inactivation of vGlut2, further supporting the notion that VTA-DAT neurons and PM_V-DAT neurons operate through distinct neurotransmitter systems in different behavioral contexts.

Direct optogenetic stimulation of all neurons or a specific subpopulation of neurons within the VMH_{VL} results in robust aggressive posturing in resident male mice toward intruders (Lin et al., 2011; Lee et al., 2014) and toward inanimate objects (Lin et al., 2011). Optogenetic stimulation of excitatory neurons of the MeA, many of which project to the VMH_{VL}, also increases male aggressive behavior (Hong et al., 2014), and similar results have been reported for stimulation of a subpopulation of aromatase neurons in the MeA (Unger et al., 2015). We have found that PM_V-DAT inputs to target structures, including the VMH_{VL}, are principally excitatory and are most effective at high-fidelity synaptic transmission at low frequencies. Stimulation of PM_V-DAT neurons promotes social exploration, but not aggression, and does not evoke aggression toward inanimate objects. Thus, we propose that social behavior engaged by PM_V-DAT neurons is tightly controlled to promote social exploration without escalating to aggression.

Isolation of mRNA associated with polyribosomes from DAT-expressing neurons of the PM_V reveals that these cells are highly enriched for dopaminergic markers compared to cells in the surrounding tissue, making them the only known population to contain mRNA for all dopaminergic markers, but not to release detectable dopamine. A likely explanation for our inability to detect dopamine release from these neurons is that while these neurons do contain mRNA for the molecular machinery to synthesize and release this neurotransmitter, their mRNA levels are an order of magnitude less than those in conventional VTA-DAT neurons. Why neurons in the PM_V contain any mRNA at all for dopaminergic enzymes is not clear. One possibility is that these neurons are derived from a common lineage of other dopamine neurons in the hypothalamus and midbrain that express these markers, but the mRNA in PM_V-DAT neurons is not translated into protein or these proteins are rapidly degraded and thus are in quantities below the level of detection. A second possibility is that these neurons utilize dopamine as a neurotransmitter early during development and then switch to glutamatergic once circuit connectivity is established, while maintaining residual dopaminergic mRNA expression following this switch. Evidence for developmental neurotransmitter switching has been widely reported (Spitzer, 2015). A third possibility is that these neurons have the capacity to enhance dopamine production and release under specific environmental demands. Neurotransmitter switching has been previously reported in the adult hypothalamus (Dulcis et al., 2013). Future experiments designed to determine the relevance of dopamine marker mRNA expression in PM_V-DAT neurons will further inform the identity and function of the unique neuronal population.

EXPERIMENTAL PROCEDURES

See the Supplemental Experimental Procedures for additional experimental procedures.

Mice

All procedures were approved and conducted in accordance with the guidelines of the Institutional Animal Care and Use Committee of the University of Washington. Mice 8 weeks or older were used for all experiments, except for slice electrophysiology, where 5- to 8-week-old mice were used.

RiboTag

Immunoprecipitation was performed as described previously (Sanz et al., 2009). Briefly, 1 × 1 mm punches of PM_V and VTA were removed, homogenized, and incubated with anti-HA antibody (Covance), coupled to magnetic beads (Pierce) overnight at 4°C. Following elution from magnetic beads, RNA from both IP and input samples was obtained using the RNeasy micro kit (QIAGEN). cDNA was generated using oligo dT primers (Invitrogen). TaqMan (Applied Biosystems) primers were used for qRT-PCR analysis.

Electrophysiology and Voltammetry

Whole-cell recordings were made using an Axopatch 700B amplifier (Molecular Devices). Light-evoked synaptic transmission was induced with 5-ms light pulses delivered from an optic fiber placed in the bath directly. I_h currents were induced by 2-s hyperpolarizing voltage steps from −70 to −120 mV. SK currents were induced by depolarizing voltage steps from −70 to 0 mV. Capacitance measurements were calculated by Clampex software using 5-mV

(C) Social investigation of resident animal by intruder (experimental) was decreased following inhibition of PM_V-DAT neurons by CNO/hM4Di (n = 10–11 mice/group; two-way repeated-measures ANOVA virus × CNO $F_{(1,19)} = 4.43$, $p < 0.05$; Bonferroni multiple comparisons *$p < 0.05$).
(D and E) Inhibition of PM_V-DAT neurons did not affect the investigation of a male (D) or female (E) intruder by a resident (experimental).
(F) Inhibition of PM_V-DAT neurons by CNO/hM4Di did not affect preference for a mouse over an object.
(G) Inhibition of PM_V-DAT neurons eliminated the preference for a novel mouse versus a familiar mouse; n = 10–11 mice/group; two-way repeated-measures ANOVA: $F_{(1,19)} = 7.38$, $p < 0.05$; Bonferroni multiple comparisons: *$p < 0.05$). Data are represented as mean ± SEM.
See also Figure S3.

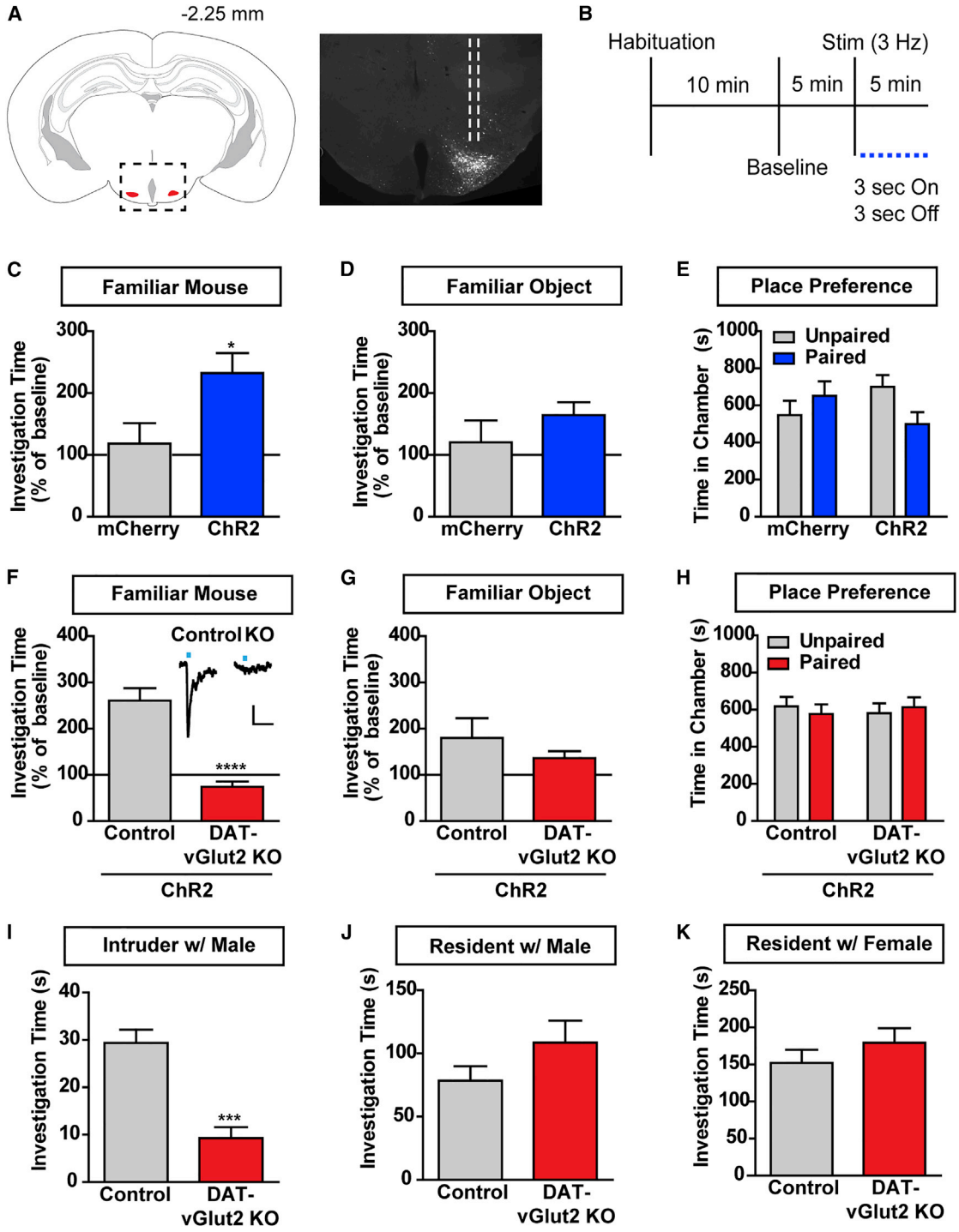

Figure 4. PM_V-DAT Neurons Regulate Social Behaviors through Glutamate Release

(A) Atlas and histology images showing ChR2-mCherry expression in the PM_V; dashed lines indicate track mark from fiber optic.

(B) Schematic of cohabitation behavioral assay.

(C) Activation of PM_V-DAT neurons increased social investigation of a familiar cage mate (n = 6–8 animals/group; Student's t test *$p < 0.05$).

(D) Activation did not increase investigation of a familiar object.

(E) Pairing one side of a two-chambered box with light stimulation did not lead to a significant preference for either side.

(F) Inactivation of vGlut2 in DAT-vGlut2 KO mice eliminates light-evoked excitatory currents driven by ChR2 expression in DAT-PM_V neurons and recorded in VMH_{VL} (inset). Light activation of PM_V-DAT neurons expressing ChR2 increased social investigation of a cage mate in DAT-vGlut2 heterozygous animals (control), but not in DAT-vGlut2 knockout animals (n = 6 animals/group; Student's t test ****$p < 0.0001$).

(legend continued on next page)

hyperpolarizing steps. Fast-scan cyclic voltammetry was performed using carbon-fiber microelectrodes as described previously (Clark et al., 2010). 5-ms light stimuli were delivered as described for electrophysiology.

Fos Induction

For social encounters, mice were assigned to the resident, intruder, or control condition. Resident animals were singly housed for at least 2 weeks, while intruder and control mice were group housed. Animals experienced a 20-min social encounter with an appropriately matched resident or intruder animal and were euthanized and perfused 90 min following the start of the encounter. Control animals remained in their home cage. Fos-positive neurons were identified and automatically counted using ImageJ software. Virally transduced DAT neurons and Fos-positive DAT neurons were counted by hand by an experienced investigator blind to the condition.

Behavior

For resident/intruder encounters, resident mice were singly housed for at least 2 weeks, were sexually experienced, and were 3–4 weeks older than intruder animals, which were group housed. Saline or CNO (1 mg/kg) was administered intraperitoneally 40 min prior to the start of the encounter. Each mouse received saline and CNO on subsequent days (order of administration was counterbalanced across groups) and encountered a different resident or intruder mouse on each day. Scored social behaviors included anogenital sniffing, oronasal sniffing, following, and grooming. For the three-chamber assay, mice were given 10 min to explore the empty arena and then were briefly returned to their home cage, while the novel object (empty wire pencil cup) was introduced to one chamber. The first mouse (contained in a wire pencil cup) was introduced to the opposite chamber, and the experimental animal was returned to the arena for a 10-min exploration and then briefly removed again, while the novel mouse was added, before a final 10-min exploration. The first 5 min of each exploration period was scored for the time spent in each chamber. For home-cage social encounters, mice implanted with fiber optics were housed with a single littermate. After the implanted mouse was connected to the fiber optic cable, they were allowed a 10-min habituation period, which was not scored, followed by a 5-min baseline period and 5 min of light stimulation (3 Hz, 5 ms, 3 s on, 3 s off).

SUPPLEMENTAL INFORMATION

Supplemental Information includes Supplemental Experimental Procedures and four figures and can be found with this article online at http://dx.doi.org/10.1016/j.celrep.2016.05.067.

AUTHOR CONTRIBUTIONS

M.E.S. performed the electrophysiology, behavior, and histology experiments. S.M.M. performed the RiboTag experiments and assisted with behavior. L.M.B. and M.E.S. performed the voltammetry experiments. P.E.M.P. and T.S.H. provided resources. M.E.S. and L.S.Z. designed the experiments and wrote the paper.

ACKNOWLEDGMENTS

The authors wish to thank Drs. Richard Palmiter and Stephanie Padilla for helpful discussion and comments on the manuscript, Dr. Christina Sanford for providing the Python script used for projection analysis, and Cerise Knakal for technical assistance. This work was supported by the NIH (R01-MH094536 to L.S.Z, P50-MH106428-5877 to P.E.M.P., and R01-DA036612 to T.S.H).

Received: January 25, 2016
Revised: April 22, 2016
Accepted: May 17, 2016
Published: June 23, 2016

REFERENCES

Armbruster, B.N., Li, X., Pausch, M.H., Herlitze, S., and Roth, B.L. (2007). Evolving the lock to fit the key to create a family of G protein-coupled receptors potently activated by an inert ligand. Proc. Natl. Acad. Sci. USA *104*, 5163–5168.

Borelli, K.G., Blanchard, D.C., Javier, L.K., Defensor, E.B., Brandão, M.L., and Blanchard, R.J. (2009). Neural correlates of scent marking behavior in C57BL/6J mice: detection and recognition of a social stimulus. Neuroscience *162*, 914–923.

Canteras, N.S., Simerly, R.B., and Swanson, L.W. (1992). Projections of the ventral premammillary nucleus. J. Comp. Neurol. *324*, 195–212.

Cavalcante, J.C., Bittencourt, J.C., and Elias, C.F. (2006). Female odors stimulate CART neurons in the ventral premammillary nucleus of male rats. Physiol. Behav. *88*, 160–166.

Cavalcante, J.C., Bittencourt, J.C., and Elias, C.F. (2014). Distribution of the neuronal inputs to the ventral premammillary nucleus of male and female rats. Brain Res. *1582*, 77–90.

Choi, G.B., Dong, H.W., Murphy, A.J., Valenzuela, D.M., Yancopoulos, G.D., Swanson, L.W., and Anderson, D.J. (2005). Lhx6 delineates a pathway mediating innate reproductive behaviors from the amygdala to the hypothalamus. Neuron *46*, 647–660.

Clark, J.J., Sandberg, S.G., Wanat, M.J., Gan, J.O., Horne, E.A., Hart, A.S., Akers, C.A., Parker, J.G., Willuhn, I., Martinez, V., et al. (2010). Chronic microsensors for longitudinal, subsecond dopamine detection in behaving animals. Nat. Methods *7*, 126–129.

Donato, J., Jr., Cavalcante, J.C., Silva, R.J., Teixeira, A.S., Bittencourt, J.C., and Elias, C.F. (2010). Male and female odors induce Fos expression in chemically defined neuronal population. Physiol. Behav. *99*, 67–77.

Donato, J., Jr., Lee, C., Ratra, D.V., Franci, C.R., Canteras, N.S., and Elias, C.F. (2013). Lesions of the ventral premammillary nucleus disrupt the dynamic changes in Kiss1 and GnRH expression characteristic of the proestrus-estrus transition. Neuroscience *241*, 67–79.

Dulcis, D., Jamshidi, P., Leutgeb, S., and Spitzer, N.C. (2013). Neurotransmitter switching in the adult brain regulates behavior. Science *340*, 449–453.

Gunaydin, L.A., Grosenick, L., Finkelstein, J.C., Kauvar, I.V., Fenno, L.E., Adhikari, A., Lammel, S., Mirzabekov, J.J., Airan, R.D., Zalocusky, K.A., et al. (2014). Natural neural projection dynamics underlying social behavior. Cell *157*, 1535–1551.

Hedreen, J. (1978). Neuronal degeneration caused by lateral ventricular injection of 6-hydroxy-dopamine. I. The ventral premammillary nucleus and other cell groups. Brain Res. *157*, 129–135.

Hnasko, T.S., Chuhma, N., Zhang, H., Goh, G.Y., Sulzer, D., Palmiter, R.D., Rayport, S., and Edwards, R.H. (2010). Vesicular glutamate transport promotes dopamine storage and glutamate corelease in vivo. Neuron *65*, 643–656.

Hong, W., Kim, D.W., and Anderson, D.J. (2014). Antagonistic control of social versus repetitive self-grooming behaviors by separable amygdala neuronal subsets. Cell *158*, 1348–1361.

Kevetter, G.A., and Winans, S.S. (1981). Connections of the corticomedial amygdala in the golden hamster. II. Efferents of the "olfactory amygdala". J. Comp. Neurol. *197*, 99–111.

(G) Activation did not increase investigation of a familiar object in either group.
(H) Pairing one side of a two-chambered box with light stimulation did not cause a significant preference in either group.
(I) Social investigation of a resident male by an intruder male was reduced in DAT-vGlut2 knockout animals (n = 6 animals/group; Student's t test ***$p < 0.001$).
(J and K) Social investigation of a male (J) or female (K) intruder by a resident was unaffected. Data are represented as mean ± SEM.
See also Figure S4.

Please cite this article in press as: Soden et al., Genetic Isolation of Hypothalamic Neurons that Regulate Context-Specific Male Social Behavior, Cell Reports (2016), http://dx.doi.org/10.1016/j.celrep.2016.05.067

Lammel, S., Steinberg, E.E., Földy, C., Wall, N.R., Beier, K., Luo, L., and Malenka, R.C. (2015). Diversity of transgenic mouse models for selective targeting of midbrain dopamine neurons. Neuron *85*, 429–438.

Lee, H., Kim, D.W., Remedios, R., Anthony, T.E., Chang, A., Madisen, L., Zeng, H., and Anderson, D.J. (2014). Scalable control of mounting and attack by Esr1+ neurons in the ventromedial hypothalamus. Nature *509*, 627–632.

Lein, E.S., Hawrylycz, M.J., Ao, N., Ayres, M., Bensinger, A., Bernard, A., Boe, A.F., Boguski, M.S., Brockway, K.S., Byrnes, E.J., et al. (2007). Genome-wide atlas of gene expression in the adult mouse brain. Nature *445*, 168–176.

Leshan, R.L., Louis, G.W., Jo, Y.H., Rhodes, C.J., Münzberg, H., and Myers, M.G., Jr. (2009). Direct innervation of GnRH neurons by metabolic- and sexual odorant-sensing leptin receptor neurons in the hypothalamic ventral premammillary nucleus. J. Neurosci. *29*, 3138–3147.

Lin, D., Boyle, M.P., Dollar, P., Lee, H., Lein, E.S., Perona, P., and Anderson, D.J. (2011). Functional identification of an aggression locus in the mouse hypothalamus. Nature *470*, 221–226.

Meister, B., and Elde, R. (1993). Dopamine transporter mRNA in neurons of the rat hypothalamus. Neuroendocrinology *58*, 388–395.

Motta, S.C., Goto, M., Gouveia, F.V., Baldo, M.V., Canteras, N.S., and Swanson, L.W. (2009). Dissecting the brain's fear system reveals the hypothalamus is critical for responding in subordinate conspecific intruders. Proc. Natl. Acad. Sci. USA *106*, 4870–4875.

Oh, S.W., Harris, J.A., Ng, L., Winslow, B., Cain, N., Mihalas, S., Wang, Q., Lau, C., Kuan, L., Henry, A.M., et al. (2014). A mesoscale connectome of the mouse brain. Nature *508*, 207–214.

Sanz, E., Yang, L., Su, T., Morris, D.R., McKnight, G.S., and Amieux, P.S. (2009). Cell-type-specific isolation of ribosome-associated mRNA from complex tissues. Proc. Natl. Acad. Sci. USA *106*, 13939–13944.

Scalia, F., and Winans, S.S. (1975). The differential projections of the olfactory bulb and accessory olfactory bulb in mammals. J. Comp. Neurol. *161*, 31–55.

Sosulski, D.L., Bloom, M.L., Cutforth, T., Axel, R., and Datta, S.R. (2011). Distinct representations of olfactory information in different cortical centres. Nature *472*, 213–216.

Spitzer, N.C. (2015). Neurotransmitter Switching? No Surprise. Neuron *86*, 1131–1144.

Swanson, L.W. (2000). Cerebral hemisphere regulation of motivated behavior. Brain Res. *886*, 113–164.

Unger, E.K., Burke, K.J., Jr., Yang, C.F., Bender, K.J., Fuller, P.M., and Shah, N.M. (2015). Medial amygdalar aromatase neurons regulate aggression in both sexes. Cell Rep. *10*, 453–462.

Vandenberg, M.J., Terhorst, G.J., and Koolhaas, J.M. (1983). The nucleus premammillaris ventralis (Pmv) and aggressive-behavior in the rat. Aggress. Behav. *9*, 41–47.

Wu, Z., Autry, A.E., Bergan, J.F., Watabe-Uchida, M., and Dulac, C.G. (2014). Galanin neurons in the medial preoptic area govern parental behaviour. Nature *509*, 325–330.

Yoon, H., Enquist, L.W., and Dulac, C. (2005). Olfactory inputs to hypothalamic neurons controlling reproduction and fertility. Cell *123*, 669–682.

Yu, Q., Teixeira, C.M., Mahadevia, D., Huang, Y., Balsam, D., Mann, J.J., Gingrich, J.A., and Ansorge, M.S. (2014). Dopamine and serotonin signaling during two sensitive developmental periods differentially impact adult aggressive and affective behaviors in mice. Mol. Psychiatry *19*, 688–698.

Zhuang, X., Masson, J., Gingrich, J.A., Rayport, S., and Hen, R. (2005). Targeted gene expression in dopamine and serotonin neurons of the mouse brain. J. Neurosci. Methods *143*, 27–32.

Zoli, M., Agnati, L.F., Tinner, B., Steinbusch, H.W., and Fuxe, K. (1993). Distribution of dopamine-immunoreactive neurons and their relationships to transmitter and hypothalamic hormone-immunoreactive neuronal systems in the rat mediobasal hypothalamus. A morphometric and microdensitometric analysis. J. Chem. Neuroanat. *6*, 293–310.

Cell Reports, Volume *16*

Supplemental Information

Genetic Isolation of Hypothalamic Neurons that Regulate Context-Specific Male Social Behavior

Marta E. Soden, Samara M. Miller, Lauren M. Burgeno, Paul E.M. Phillips, Thomas S. Hnasko, and Larry S. Zweifel

Figure S1, Related to Figure 1

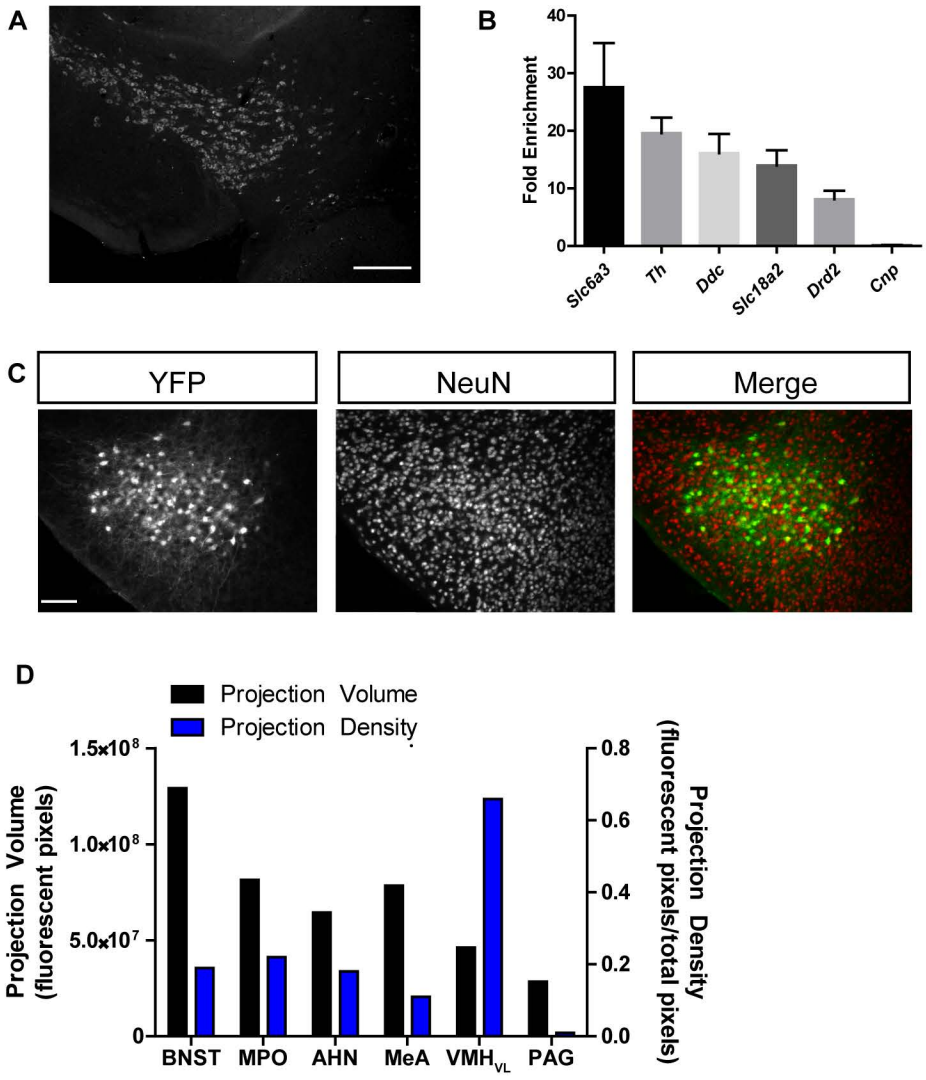

Figure S1.
(A) Immunohistochemistry for Rpl22-HA in DAT neurons of the VTA. Scale bar: 250 µm. (B) Fold enrichment (IP compared to input) of specific mRNAs isolated from VTA-DAT neurons. Data are represented as mean ± SEM. (C) Immunohistochemistry in the PMv for DAT neurons expressing YFP and the neuronal marker NeuN. Scale bar: 100 µm. (D) Quantification of DAT-PM_V projections utilizing data from the Allen Brain Institute Connectivity Atlas. Projection Volume = total fluorescent pixels from labeled axon fibers in the indicated target structure. Projection Density = fluorescent pixels normalized to the total number of pixels in the target structure.

Figure S2, Related to Figure 2

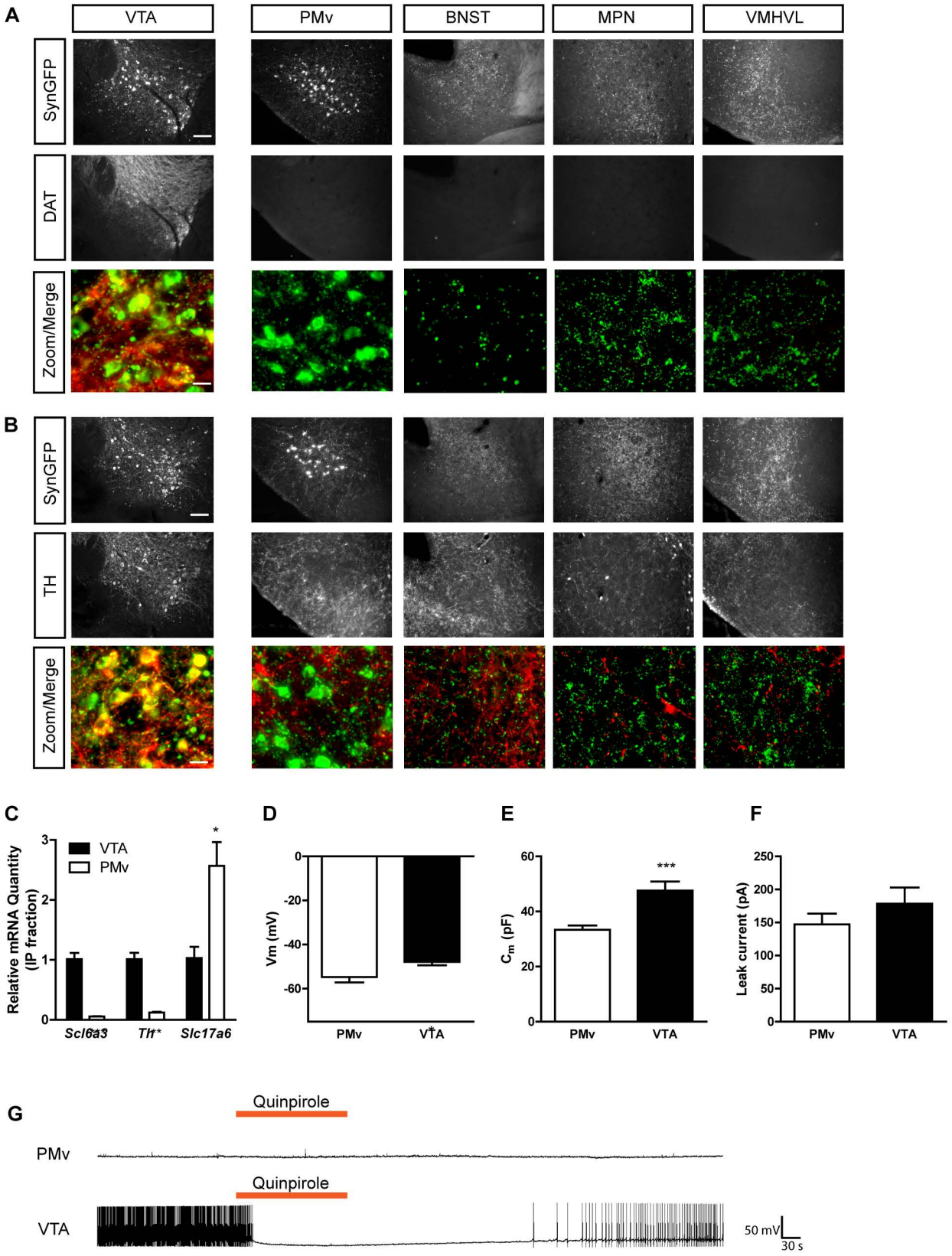

Figure S2.
Immunostaining for DAT (A) and TH (B) revealed no detectable protein in PMv-DAT cell bodies or projections, though staining was readily apparent in VTA cell bodies. TH protein was found in the vicinity of many synaptoGFP-labeled fibers in some areas, but no overlap was observed (see zoom and merge of representative regions). Scale bar: 100 μm; scale bar for zoom/merge: 10 μm. (C) Comparison of relative mRNA quantity for the indicated transcripts isolated from DAT-expressing neurons in the PMv or VTA. (D) Vm was significantly more depolarized in VTA-DAT neurons compared to PMv-DAT neurons. (E) Cm was significantly higher in VTA-DAT neruons compared to PMv-DAT neurons. (F) Leak current measured during hyperpolarizing voltage steps was unchanged. (G) Quinpirole hyperpolarized and reduced firing in VTA-DAT neurons, but had no noticable effect on PMv-DAT neurons. For all panels: Student's t test: *$p<0.05$, **$p<0.01$, ***$p<0.001$. Data are represented as mean ± SEM.

Figure S3, Related to Figure 3

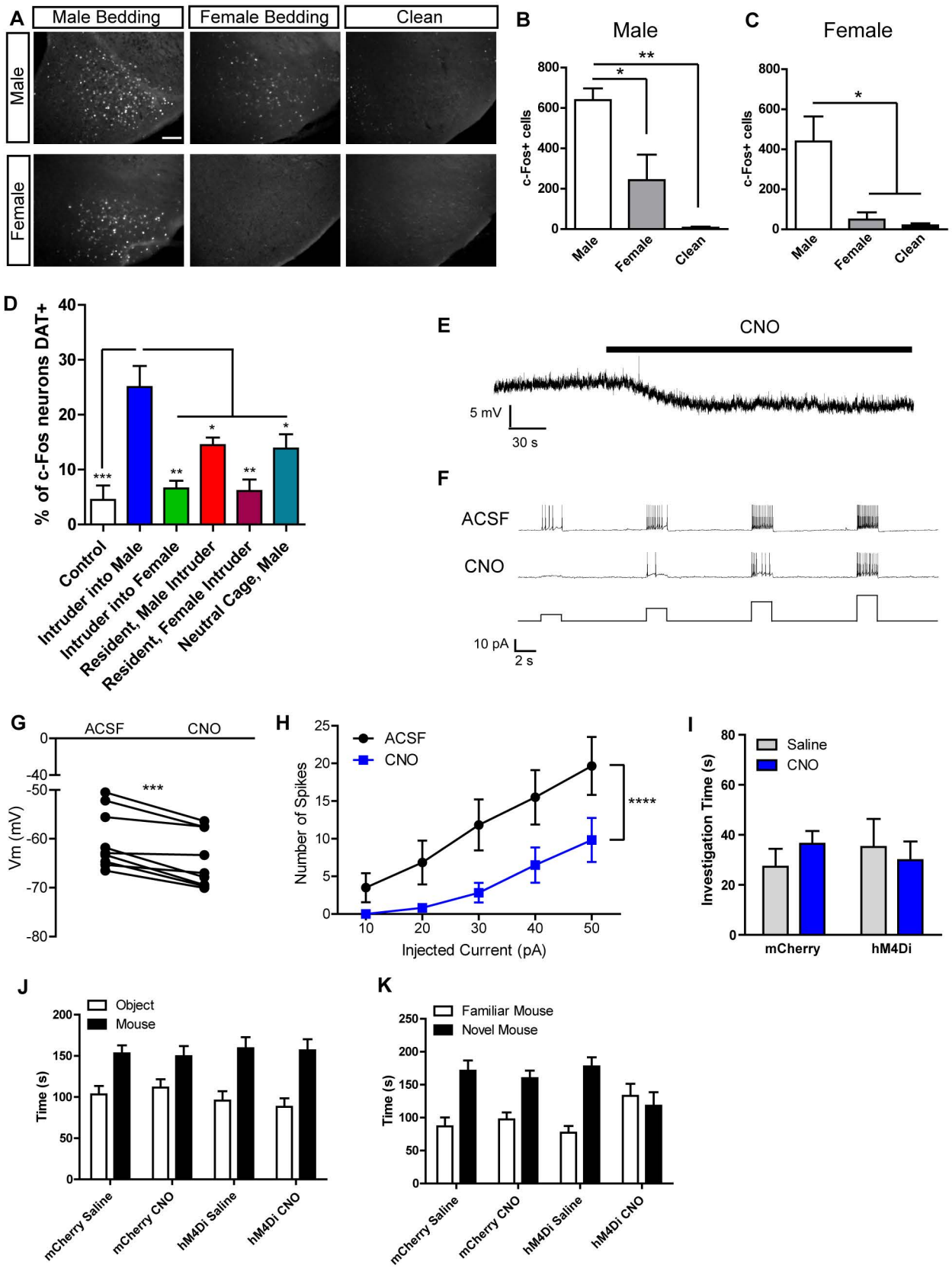

Figure S3.
(A) Immunostaining for Fos reveals activation of the PMv in male mice when exposed to male or female odorants (soiled bedding) and in female mice when exposed to male odorants. Scale bar: 100 µm. (B-C) Quantification of Fos-positive cells after odorant exposure. (n=3-4 mice/group; one-way ANOVA, Male: $F_{(2,6)}$ = 15.94, p<0.01, Female: $F_{(2,8)}$ =8.132, p<0.05). (D) The percent of Fos+ neurons also YFP labeled (DAT-Cre+) following social encounter. (n=3 mice/group; One-way ANOVA; $F_{(5,12)}$ = 9.829, p<0.001; for panels B-D: Tukey's Multiple Comparison Test: *p<0.05, **p<0.01, ***p<0.001). (E-F) Example traces showing hyperpolarization (E) and reduced excitability during current injection (F) following bath CNO application in hM4D-YFP-expressing PMv-DAT neurons. (G) Quantification of change in Vm following CNO application.(n=9 cells, paired t-test, ***p<0.001.) (H) Number of spikes elicited by 2 second current injection before and after CNO application. (n=6 cells, 2-way repeated measures ANOVA, $F_{(1,25)}$=51.35, ****p<0.0001.) (I) Inhibition of PMv-DAT neurons did not affect investigation time during a neutral cage encounter (n=6 mice/group). (J-K) Time spent in each chamber of the 3-chamber assay during Trial 1 (J) and Trial 2 (K). Data are represented as mean ± SEM.

Figure S4, Related to Figure 4

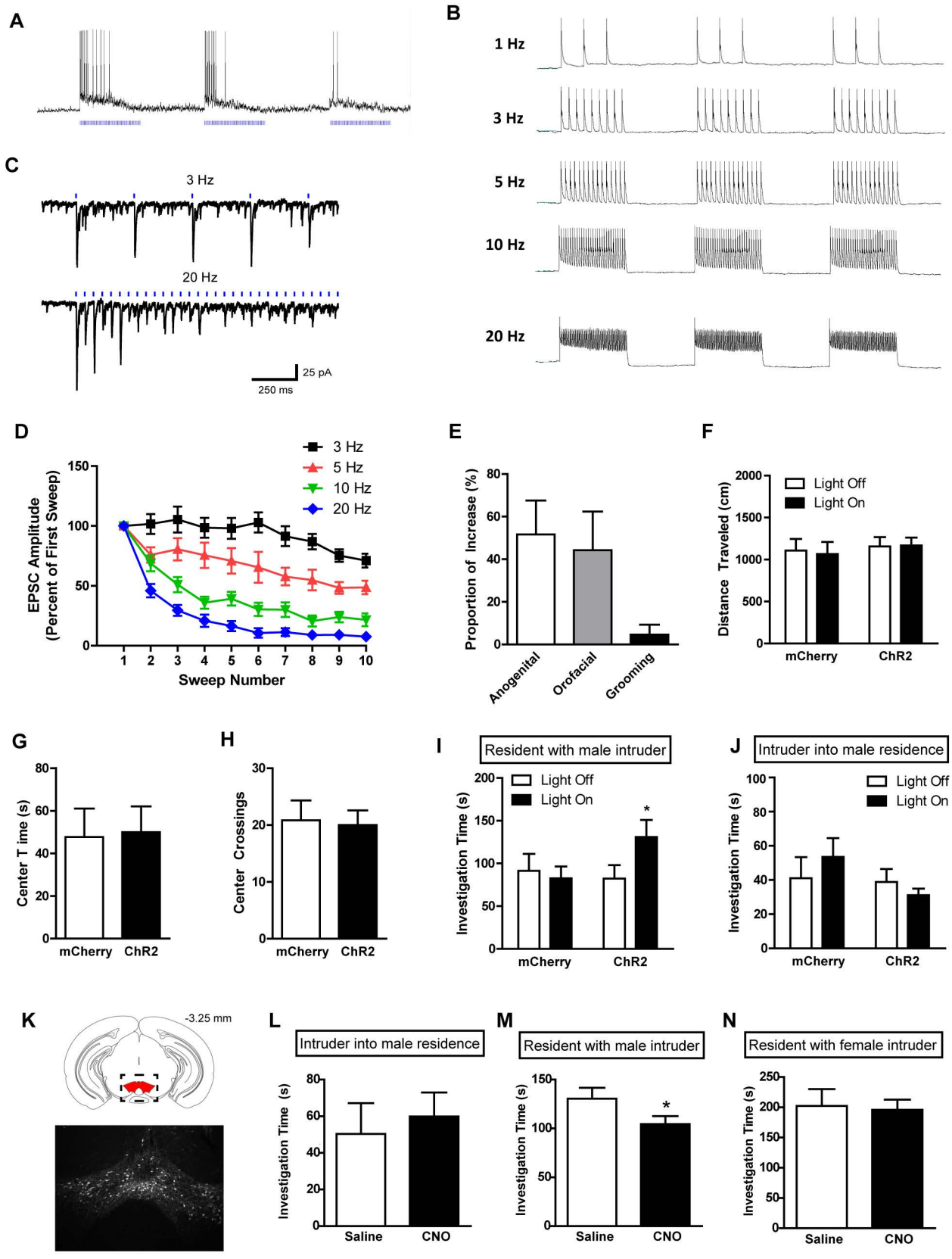

Figure S4.
(A) Example trace from a VMH_{VL} neuron showing reduced excitation following repeated bouts of 20 Hz stimulation of incoming PMv-DAT fibers expressing ChR2. (B) Example traces of light-evoked action potentials in a PMv-DAT neuron at various frequencies. (C) Example traces from recordings in the VMH_{VL} showing light-evoked EPSCs during the beginning of the first sweep at 3 or 20 Hz, illustrating significant rundown at the higher frequency. (D) Quantification of the average EPSC amplitude (first 5 events/sweep) across sweeps; each sweep was 3 seconds of light stimulation at the indicated frequency followed by 3 seconds of light off between sweeps (n=12 cells; 2-way repeated measures ANOVA Frequency x Sweep: $F_{(36, 440)}$=2.68, p<0.0001). (E) Proportion of the increased investigation time in ChR2 animals during the co-habitation assay that was attributed to each type of investigation. (F) Distance traveled was unaffected by light stimulation during the co-habitation assay. (G-H) Time spent in the center of an open field and number of center crossings were not affected by light stimulation in ChR2 vs control animals. (I) Light stimulation of PMv-DAT neurons expressing ChR2 during a standard resident-intruder assay increased investigation time by a resident animal compared to mCherry control (n=6 mice/group; 2-way repeated measures ANOVA Virus x Light: $F_{(1,10)}$=5.03, p<0.05. Bonferroni Multiple Comparisons *p<0.05). (J) Light stimulation of PMv-DAT neurons in intruder animals had no effect on investigation time. (K) Atlas image (top) and representative histology image (bottom) showing hM4Di-YFP expression in the VTA. Scale bar: 250 µm. (L) Social investigation of a resident male by an intruder male was unaffected by CNO/hM4Di inhibition of VTA-DAT neurons. (M) Social investigation of a male intruder by a resident male was decreased by VTA-DAT neuron inhibition (n=8 animals/group; Paired t test *p<0.05). (N) Social investigation of a female intruder was unaffected. Data are represented as mean ± SEM.

Supplemental Experimental Procedures

Mice

All procedures were approved and conducted in accordance to the guidelines of the Institutional Animal Care and Use Committee of the University of Washington. All mice were on a C57BL/6J background. *Slc6a3*$^{Cre/+}$ (DAT-Cre) mice were as described (Zhuang et al., 2005). *Rpl22*$^{HA/+}$ (RiboTag) mice were as described (Sanz et al., 2009). *Slc17a6*$^{lox/lox}$ (vGlut2 lox) mice were as described (Hnasko et al., 2010); these mice were crossed with *Slc6a3*$^{icre/+}$ mice (DAT-ires-Cre; Backman et al., 2006; Jackson Labs: B6.SJL-Slc6a3tm1.1(cre)Bkmn/J) to generate DAT-vGlut2 knockout animals (*Slc17a6*$^{lox/lox}$; *Slc6a3*$^{icre/+}$). Control mice were *Slc17a6*$^{lox/+}$; *Slc6a3*$^{icre/+}$. Mice were housed under a 12-hour light-dark cycle with ad libitum food and water access. Mice 8 weeks or older were used for all experiments except slice electrophysiology, where 5- to 8-week-old mice were used. See table below for age and weight ranges and housing conditions for all behavioral experiments. All interacting animals were wild-type C57BL/6J.

Experiment(s)	Figure	Experimental Animal			Interacting Animal		
		Age Range	Weight Range	Housing Condition	Age Range	Weight Range	Housing Condition
Social Encounter Fos, Resident/Intruder	3, 4	12-14 wks (Resident)	27-29g	Single	8-10 wks	23-25g (male) 20-24g (female)	Grouped
		8-10 wks (Intruder)	23-25g	Grouped	12-14 wks (male), 10-12 wks (female)	27-29g (male), 22-24g (female)	Single
3 Chamber	3	10-12 wks	25-27g	Grouped	8-10 wks	23-25g	Grouped
Co-habitation, object, RTPP, open field	4	10-12 wks	25-27g	Grouped	10-12 wks	25-27g	Grouped

Viruses

All AAV viruses were produced in house with titers of 1-3 x10^{12} particles per mL as described (Gore et al., 2013).

Surgery

Mice were anesthetized with isoflurane before injection of AAV. Coordinates for the PM_V were intentionally rostral to avoid infecting DAT cells in the midbrain (from bregma in mm, A-P: -1.9, M-L: ±0.5, D-V: -5.4). Coordinates for the VTA were deliberately caudal to avoid infecting DAT

cells in the PMV (from bregma in mm, A-P: -3.75, M-L: ±0.5, D-V: -4.5). For in vivo ChR2 experiments mice were injected unilaterally and implanted with fiber optic cannulae manufactured in house as described (Sparta et al., 2012) (from bregma in mm, A-P: -2.3, M-L: -+0.5, D-V: -5.0). Recovery was allowed for 2 weeks prior to behavioral testing or slice electrophysiology. Correct injection sites were confirmed using immunohistochemistry on brain tissue sections collected after behavioral testing. Only mice with correct targeting were included.

Immunohistochemistry

Primary antibodies were against GFP (mouse, 1:1000, Invitrogen A11120; or rabbit, 1:1000, Invitrogen A11122), c-Fos (rabbit, 1:2000, Millipore ABE457) TH (mouse, 1:1000, Millipore MAB318), DAT (rat, 1:1000, Millipore, MAB369), HA (mouse, 1:1000, ABM G036), or NeuN (rabbit, 1:2000, AbCam 177487). Secondary antibodies were conjugated to DyLight488 or CY3 (1:250, Jackson Immunolabs). All staining was done on free-floating sections (overnight primary incubation at 4°C), with the exception of DAT,TH, and HA staining, for which sections were mounted on slides and boiled for 20 min in antigen retrieval solution (10 mM sodium citrate, 0.05% Tween 20, pH 6.0) prior to staining (48-hr primary incubation at 4°C).

RiboTag

Immunoprecipitation was performed as described previously (Sanz et al., 2009). Briefly, 1 mm x 1 mm punches of PM_V and VTA were removed and flash-frozen. Tissue from 2-3 animals was pooled and homogenized and incubated with 5 µl of anti-HA antibody (Covance) coupled to 200 µl of magnetic beads (Pierce) overnight at 4°C. Following elution from magnetic beads, RNA from both immunoprecipitated (IP) samples and input samples was obtained using the RNeasy micro kit (Qiagen) according to manufacturer's directions. Total RNA was quantified using a Ribogreen RNA assay kit (Invitrogen). cDNA was generated using oligo dT primers from equal amounts of starting RNA, according to manufacturer protocol (Invitrogen). For qRT-PCR analysis, TaqMan (Applied Biosystems) primers were used to detect gene expression levels. Dopamine markers tested were: *Slc6a3* (dopamine transporter), *Th* (tyrosine hydroxylase), *Ddc* (dopa decarboxylase), *Slc18a2* (vesicular monoamine transporter), and *Drd2* (dopamine receptor D2). The glial marker *Cnp* (2',3'-cyclic nucleotide 3' phosphodiesterase) was used as a negative control. Relative expression values were obtained using the comparative CT method and normalized to *Actb* mRNA levels. Fold enrichment was calculated as the IP versus input ratio and represented the amount of the transcript in the targeted cell type (IP) when compared to equal amounts of RNA from the input.

Projection analysis

Projection data was obtained from the Allen Institute for Brain Science Mouse Connectivity Atlas Application Programming Interface (Oh et al., 2014; http://help.brain-map.org/display/mouseconnectivity/API). Total fluorescent pixel count and projection density (fluorescent pixel count/ total pixel count) for each defined target region in *Slc6a3*$^{Cre/+}$ mice injected in the PM_V with AAV1-FLEX-EGFP were queried using Python scripts available upon request.

Electrophysiology

Whole-cell recordings were made using an Axopatch 700B amplifier (Molecular Devices) with filtering at 1 KHz using 4-6 MΩ electrodes filled with an internal solution containing (in mM): 130 K-gluconate, 10 HEPES, 5 NaCl, 1 EGTA, 5 Mg-ATP, 0.5 Na-GTP, pH 7.3, 280 mOsm. Horizontal brain slices (200 µm) for VTA recordings and coronal brain slices (250 µm) for all other recordings were prepared from 5-8 week old mice in an ice slush solution containing (in mM): 92 NMDG, 2.5 KCl, 1.25 NaH_2PO_4, 30 $NaHCO_3$, 20 HEPES, 25 glucose, 2 thiouria, 5 Na-ascorbate, 3 Na-pyruvate, 0.5 $CaCl_2$, 10 $MgSO_4$, pH 7.3-7.4 (Ting et al., 2014). Slices recovered for ~12 min in the same solution at 32°C and then were transferred to a room temperature solution including (in mM): 92 NaCl, 2.5 KCl, 1.25 NaH_2PO_4, 30 $NaHCO_3$, 20 HEPES, 25 glucose, 2 thiouria, 5 Na-ascorbate, 3 Na-pyruvate, 2 $CaCl_2$, 2 $MgSO_4$. Slices recovered for an additional 45 min. All solutions were continually bubbled with O_2/CO_2, and all recordings were made in ACSF at 32°C continually perfused over slices at a rate of ~2 ml/min. Light-evoked synaptic transmission was induced with 5-ms light pulses delivered from an optic fiber placed directly in the bath. I_h currents were induced by 2-s hyperpolarizing voltage steps from -70 mV to -120 mV. SK currents were induced by 0.5-s depolarizing voltage steps from -70 to 0 mV. Capacitance measurements were calculated by Clampex software using 5 mV hyperpolarizing steps.

Voltammetry

Slices were prepared as described above. Fast-scan cyclic voltammetry was performed using carbon-fiber microelectrodes encased in fused-silica capillary tubing (Polymicro Technologies) as described (Clark et al., 2010). 5-ms light stimuli were delivered as described for electrophysiology. A variety of stimulus parameters were used in an attempt to measure dopamine release (5 to 100 stimuli at frequencies of 5 to 30 Hz). Example trace of successful release in the NAc from VTA fibers was elicited with 5 stimuli at 20 Hz.

Fos Induction

For odorant induction of Fos, experimental animals were singly housed and were transferred to a clean cage each day for 3 days prior to the experiment in order to acclimate the mice to cage changes. To generate soiled bedding a single wild-type male or female animal was housed in a cage with no bedding changes for one week. These animals were removed immediately prior to the experiment. Experimental animals were transferred to a cage containing soiled bedding and were perfused after 90 min.

For social encounter Fos experiments, mice were assigned to the resident, intruder, or control condition. Resident animals were singly housed for at least two weeks (final 7 days with no cage change), while intruder and control mice were group housed. Animals experienced a 20-min social encounter with an appropriately matched resident or intruder animal, and were euthanized and perfused 90 min following the start of the encounter. Control animals remained in their home cage. For the neutral cage encounter, “resident” and “intruder” animals were housed and treated as described above, but the encounter took place in a clean cage. The “resident” animal was placed in the cage first, followed by the “intruder” animal within one minute.

Fos-positive neurons were identified and counted automatically using ImageJ software. Virally transduced DAT neurons and Fos-positive DAT neurons were counted by hand by an experienced investigator blind to condition.

Behavior

For resident/intruder encounters, resident mice were singly housed for at least two weeks (final 7 days with no cage change), were sexually experienced, and were 3-4 weeks older than intruder animals, which were group housed. Female intruders were not staged for sexual receptivity. Encounters took place during the light cycle. For hM4Di experiments, saline or CNO (1 mg/kg) was administered intraperitoneally 40 min prior to the start of the encounter. Each mouse received saline and CNO on subsequent days (order of administration was counterbalanced across groups) and encountered a different resident or intruder mouse on each day. Encounters lasted for 10 min, and videos were hand scored by an experienced investigator blind to treatment. Social behaviors scored included anogenital sniffing, oronasal sniffing, following, and grooming. Overt sexual and aggressive behaviors (chasing, mounting,

cornering, tail rattle, and fighting) were not seen in intruder mice and were rarely seen in resident mice, and were not included in the scoring of “social investigation.”

For the 3-chamber assay mice were administered saline or CNO (counterbalanced) 40 min prior to the start of the experiment. The arena was a white Plexiglas box (60 cm x 30 cm x 30 cm) divided into three equal sized chambers with clear Plexiglas dividers, each with a doorway allowing the mice to freely pass between chambers. Mice were given 10 min to explore the empty arena, then were briefly removed and returned to their home cage while the novel object (empty wire pencil cup) was introduced to one chamber and the first mouse (contained in a wire pencil cup) was introduced to the opposite chamber. The experimental animal was returned to the arena for a 10-min exploration and then briefly removed again while the novel mouse was added, before a final 10-min exploration. The first 5 min of each exploration period was scored for the time spent in each chamber.

For home cage social encounters mice implanted with fiber optics were housed with a single littermate during recovery from surgery. After the implanted mouse was connected to the fiber optic cable they were allowed a 10 minute habituation period, which was not scored, followed by a 5-min baseline period and 5 min of light stimulation (3 Hz, 5 ms, 3 s on, 3 s off). For object exploration the littermate was removed and an object (50 mL conical tube lid) was placed in the cage for at least 3 hr prior to testing.

For the real-time place preference assay mice were placed in a two-chambered arena with partial walls dividing the two sides that allowed for passage of the fiber optic cable. One side of the arena had horizontal black and white stripes, while the other side had vertical stripes. One side was randomly assigned to be paired with light stimulation, while the other was unpaired. The assay lasted for 20 min.

Statistics

All statistical analyses were performed using Prism software (GraphPad). For comparison of two groups an unpaired Student’s t test was used, except where noted. For comparison of multiple groups a one-way ANOVA was used, followed by Tukey’s post hoc analysis. For comparison of two or more groups across treatment condition or time a two-way repeated measure ANOVA was used, followed by Bonferroni post-hoc analysis.

Supplemental References

Backman C. M., Malik N., Zhang Y., Shan L., Grinberg A., Hoffer B. J., Westphal H., Tomac A. C. (2006). Characterization of a mouse strain expressing Cre recombinase from the 3' untranslated region of the dopamine transporter locus. Genesis 44, 383-390.

Clark J. J., Sandberg S. G., Wanat M. J., Gan J. O., Horne E. A., Hart A. S., Akers C. A., Parker J. G., Willuhn I., Martinez V., Evans S. B., Stella N., Phillips P. E. (2010). Chronic microsensors for longitudinal, subsecond dopamine detection in behaving animals. Nat Methods 7, 126-129.

Gore B. B., Soden M. E., Zweifel L. S. (2013). Manipulating gene expression in projection-specific neuronal populations using combinatorial viral approaches. Curr Protoc Neurosci 4, 4 35 31-34 35 20.

Hnasko T. S., Chuhma N., Zhang H., Goh G. Y., Sulzer D., Palmiter R. D., Rayport S., Edwards R. H. (2010). Vesicular glutamate transport promotes dopamine storage and glutamate corelease in vivo. Neuron 65, 643-656.

Sanz E., Yang L., Su T., Morris D. R., McKnight G. S., Amieux P. S. (2009). Cell-type-specific isolation of ribosome-associated mRNA from complex tissues. Proc Natl Acad Sci U S A 106, 13939-13944.

Sparta D. R., Stamatakis A. M., Phillips J. L., Hovelso N., van Zessen R., Stuber G. D. (2012). Construction of implantable optical fibers for long-term optogenetic manipulation of neural circuits. Nat Protoc 7, 12-23.

Ting J. T., Daigle T. L., Chen Q., Feng G. (2014). Acute brain slice methods for adult and aging animals: application of targeted patch clamp analysis and optogenetics. Methods Mol Biol 1183, 221-242.

Zhuang X., Masson J., Gingrich J. A., Rayport S., Hen R. (2005). Targeted gene expression in dopamine and serotonin neurons of the mouse brain. J Neurosci Methods 143, 27-32.